

## CHAPTER 15

# INVESTIGATING LAND, OCEAN, AND ATMOSPHERE WITH MULTISPECTRAL MEASUREMENTS

### 15.1 *Introducing HYDRA*

A multispectral data analysis toolkit has been developed using freeware; it is called HYDRA - HYper-spectral data viewer for Development of Research Applications. HYDRA enables interrogation of multispectral (including hyperspectral) fields of data so that (a) pixel location and spectral measurement values (radiance or brightness temperature) can be easily displayed; (b) spectral channels can be combined in linear functions and the resulting images displayed; (c) false color images can be constructed from multiple channel combinations; (d) scatter plots of spectral channel combinations can be viewed; (e) pixels in images can be found in scatter plots and vice versa; (f) transects of measurements can be displayed, and (g) soundings of temperature and moisture as well as spectra from selected pixels can be compared.

HYDRA grew out of the necessity to provide research scientists and educators with freely available software that could be employed to display and analyze remotely sensed multispectral and hyperspectral data. When considering the design of HYDRA, the most important requirements were the software must be a) freely available to the global community, b) computer platform independent, and c) extendable. It was also important that the toolkit be coded in an easy-to-use scripting language, so that users could modify and extend the capabilities as needed. The VisAD (Visualization for Algorithm Development) Java library was selected as the basis for HYDRA. This library allows applications to be written in either Java or Jython (the Java implementation of the popular Python scripting language). The core of the VisAD library is a unified Data Model, which allows for the representation of literally any numeric data in a consistent manner. This is very important when integrating data from a variety of sources that may have different sampling topologies in space or time. The Data Model also has built-in metadata for parameters such as units and error estimates. That these metadata are an integral part of the data means they can be easily used to verify correctness of computations (the software detects invalid combinations, such as adding a temperature to a pressure) and to estimate the reliability of computations.

HYDRA is being developed using the Jython (the Java implementation of Python) scripting language. The syntax of this language is simple enough that it lends itself to easy modifications by end users who are either more familiar with scripting languages or are already competent Java programmers. Although it is a scripting language, nearly all the “heavy” computing is handled by the VisAD library, which means that performance is seldom an issue.

HYDRA has become a part of the World Meteorological Organization Virtual Laboratory for Satellite Meteorology. The training materials are available to all WMO Member countries as part of the Virtual Laboratory. An interactive training tool called VISITview has been developed at Cooperative Institute for Meteorological Satellite Studies (CIMSS) for the Virtual Institute for Satellite Integration Training (VISIT). VISITview is a platform independent distance learning and collaboration software program that allows multiple users to view the same series of images containing graphics and text with a large number of user features. HYDRA will contribute to the teletraining software that is not proprietary and is freely available. VISITview is designed to provide the instructors and students with a set of easy to use tools for creating and conducting teletraining sessions.

This chapter describes some of the procedures for displaying multispectral data using HYDRA. HYDRA is available at <http://www.ssec.wisc.edu/hydra/>. A summary of the HYDRA commands follows.

#### **HYDRA** main window

Displays a world map and shows **File**, **Load**, **Tools**, **Settings**, and **Start** at top.

**File** offers

**Exit** to closes this window

**Load** has three options

**Local Data** allows you to search local directories to find MODIS, AIRS, GOES or Meteosat data.

**Remote Data** allows you to get data from a remote server

(a) Terra or Aqua Direct Broadcast or (b) Goddard DAAC

**GOES/MSG** allows you to get geostationary satellite data from an ADDE server

After a data granule is selected HYDRA displays the infrared window (at reduced resolution 4 km for MODIS) on a world map.

**Tools** offers

**Capture Display** to save the image as a jpeg

**Settings** has

**Set Color Range** where the histogram of brightness temperatures or radiances can be adjusted to maximize contrast – the color range can be altered with a right click plus drag at either end of the color scale

**Set Color Scale** where **Color**, **Gray** and **Inverse Gray** gives choice of color, grey, or inverse grey (which produces white clouds)

The toolbar at the top enables reset, zoom in, zoom out, translate, box magnify, find location, and subset at full resolution functions

Reset (left click on reset and then click on image to restore original image)

Zoom in (left click on zoom in plus click on image enables enlargement)

Zoom out (left click on zoom out plus click on image enables far view)

Translate (left click on translate plus click on image enables moving the image within the window)

Box magnify (left click on box plus click and drag to create box for enlargement)

Find location (left click on arrow plus click on image displays location of the chosen pixel)

Subset at full resolution (left click on subset plus click and drag on image creates subset of image at full resolution; this is automatically transferred from HYDRA into the Multichannel viewer when both are engaged – data is displayed at reduced resolution by default unless subset function is used)

**Start** opens **Multichannel Viewer**

wherein the measured spectra (wavenumber on x-axis and radiance or brightness temperature on y-axis) is displayed along with a spectral band superimposed on a world map. Left click on arrow icon in the bottom toolbar allows you to see the pixel value for a given lat-lon (using left click and drag).

**Tools** menu (appears in **Multichannel Viewer** window)

**Linear Combinations** opens the **Channel Combination Tool** display where you can specify linear combinations of spectral bands a,b,c and d

(a +-x/ b) +-x/ (c +-x/ d).

**RGB** allows you to select a spectral channel for each color in the RGB display

**Transect** allows you to create a line on the image and see the temperatures or radiances along the transect. This is enabled with a shift plus right click and drag.

**Capture Display** allows you to save the image as a jpeg

**Statistics** displays the min and max values in the image

**Reference Spectrum** allows you to compare spectral measurements from two selected pixels (controlled by the arrows in the bottom toolbar)

**Settings** (on the Multi-Channel Viewer) has

**Set Color Range** where the histogram of brightness temperatures or radiances can be adjusted to maximize contrast – the color range can be altered with a right click plus drag at either end of the color scale

**BT->radiance** allowing you to toggle from brightness temperatures to radiances in the infrared spectral channels

**Projection** offers **Lambert Equal Area** or **Instrument** projections of the data on the image

**Set Color Scale** where **Color**, **Gray** and **Inverse Gray** gives choice of color, grey, or inverse grey (which produces white clouds)

**Lat/Lon Grid** can be superimposed in the image with the indicated toggle enabled

**Image Label** labels the image with the instrument and day/time of the data

The **Channel Combination Tool** offers the usual tool bar and

**Compute** to create an image of the selected linear combination (you can indicate at the bottom your preference for this linear combination to be on the x- or y-axis in the scatter plot) and displays a toolbar for image manipulations (five color boxes are available in the toolbar to select regions by boxes or curves in the image that will be displayed in the scatter plot; a left click drag in the image highlights the chosen points in the scatter plot).

**Scatter** creates a scatter plot of the chosen x- and y-axis linear combinations. Five color area boxes (or area curves) in the bottom toolbar of the scatter plot allow you to select points in the scatter plot that will be displayed in the x-axis and y-axis images; a left click drag in the scatter plot highlights the chosen points in the scatter plot and simultaneously in the x- and y-axis images. Conversely (as indicated before) left click drag in the x- or y- axis images shows the locations of the chosen pixels in the scatter plot. Each color area box (or area curve) can be erased with a left click when the color box is engaged; after erasure another area box (or area curve) can be selected for this color. The zoom capability in the scatter plot (on the bottom right of the toolbar) allows you to enlarge special features in the scatter plot and investigated them in more detail.

## 15.2 Starting HYDRA

For Windows, HYDRA can be downloaded from the web site mentioned above or from <ftp://ftp.ssec.wisc.edu/visit/hydra/>. Download the file v1.6.ms or later version in binary ftp mode, and then run it by double-clicking the file icon. The installer will ask where you wish to install the program. Accept the default, C:\Program Files\hydra. Start the program by selecting Start | All Programs | hydra | Run HYDRA. A window named “HYDRA” will appear at the top left of your display (Figure 1). A window named “Run HYDRA” will also appear (this window may be minimized, but do not close it).

For Linux, download the file “hydra\_v1.6\_linux.tar.gz” or a later version in binary ftp mode and install by entering “gzip -cd hydra\_v1.5\_linux.tar.gz| tar xvf –” at a command prompt. This will create a sub-directory named “hydra” into which everything required to run will be installed. To run HYDRA, first change directory into the 'hydra' directory, and enter “.runHydra” at the command prompt.

For Macs, OSX 10.4 (Tiger) or later, repeat the procedure above for Linux, except use the file 'hydra\_v1.6\_mac.tar.gz.' Earlier versions of Mac, 10.3 (Panther) require a separate installation of Java3D.

The HYDRA window enables you to load new files and to select regions within the current file. HYDRA is designed to read MODIS Level-1B 1KM files in HDF4 format. Files obtained from the NASA DAAC, or those produced locally by a direct broadcast ground station (including IMAPP), can also be used. The rest of this paper will use a local MODIS HDF4 file as an example.

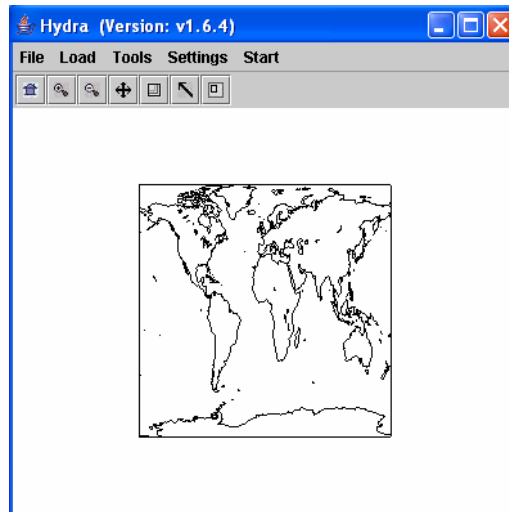


**Figure 15.1:** The “Hydra” window

The Hydra window enables you to load new files and to select regions within the current file. HYDRA is designed to read MODIS Level-1B 1KM files in HDF format. Files obtained from the NASA DAAC, or those produced locally by a direct broadcast ground station (including IMAPP), can also be used.

#### 15.2.1 Loading data

To load a MODIS Level-1B 1KM file from disk, click on “data | local” and select the file to be loaded (e.g., MYD021KM.A2001149.1030.003.2001154234131.hdf) as shown in Figure 15.2.

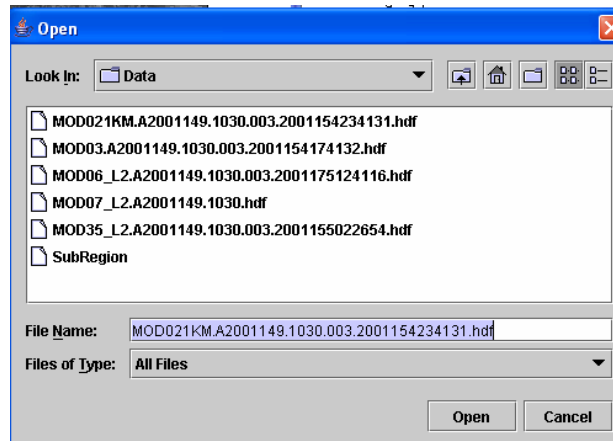


**Figure 15.2:** Loading a MODIS Level-1B 1KM file from disk

When the file is loaded, an image of the band 31 (11 micron) radiance should appear, as shown in Figure 15.3.

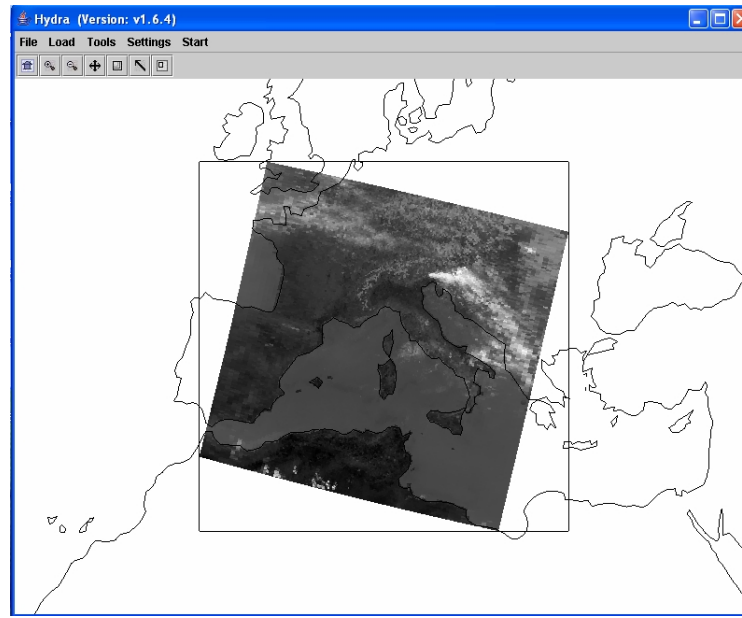


**Figure 15.3:** “Hydra” window with a MODIS L1B 1KM file loaded

### 15.2.2 Multichannel Viewing

The Multi-Channel Viewer allows you to select different spectral bands and regions from an open MODIS L1B 1KM file.

To start the Multi-Channel viewers, click on “start | Multi-Channel Viewer”. A new window should appear displaying band 31 radiance, as shown in Figure 15.4.

To select a different band, use the “Band” selector. Try band 2 (visible) and band 27 (water vapor).

Images are displayed in reflectance (for visible) and brightness temperature (for infrared) units are displayed by default. To change to radiance for visible and infrared bands, select “Settings | BT -> radiance”. From then on, all images in this window will be displayed in the selected units.

To zoom in on the image, left click on zoom (second from left on tool bar) and then click anywhere on the image. Repeat clicking on the image until desired zoom has been achieved. To pull back (zoom out), left click on far view (third from left on tool bar) and then click anywhere on the image. Repeat until desired far view is achieved.

To translate the image, left click on translate (third from right) plus click on image enables moving the image within the window, and move the cursor. The image should translate in the direction you move the cursor.

To close the top panel of the Multi-Channel Viewer, click on the left “up” pointer in the divider bar between the top and bottom panels.

Note that you can open more than one Multi-Channel Viewer window.

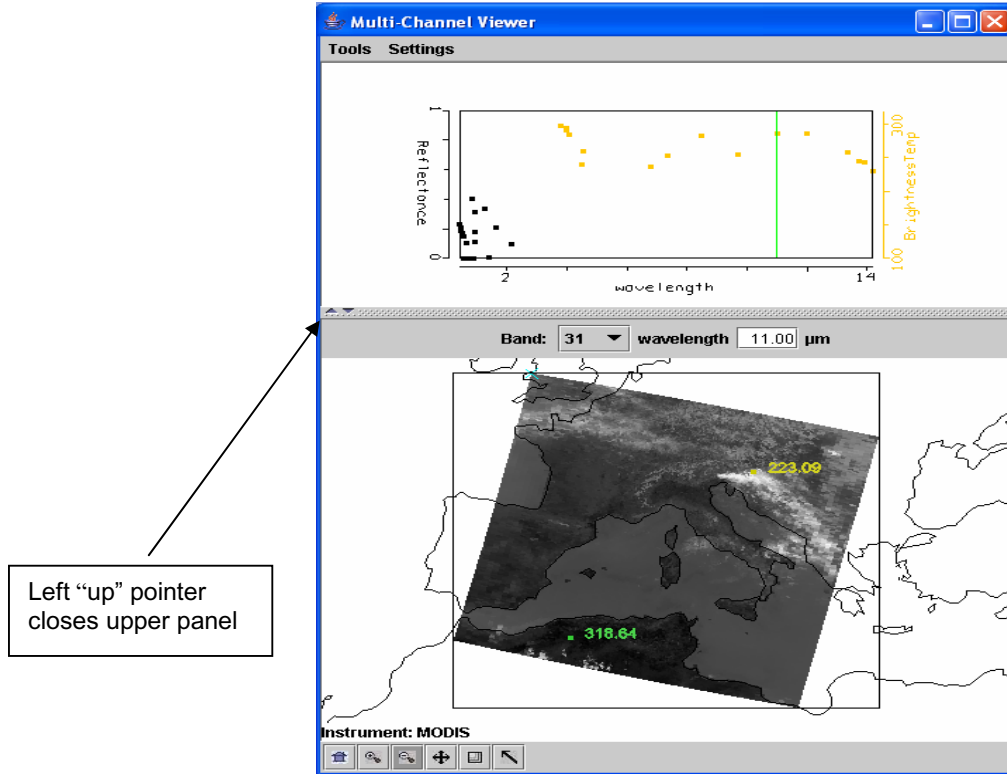


Figure 15.4: "Multi-Channel Viewer" window

15.2.3 Full resolution MODIS 1KM data

The MODIS images seen so far in HYDRA have all been at reduced resolution. To view the MODIS data at full resolution, click on the rightmost button at the bottom of the "Hydra" window, as shown in Figure 15.5.

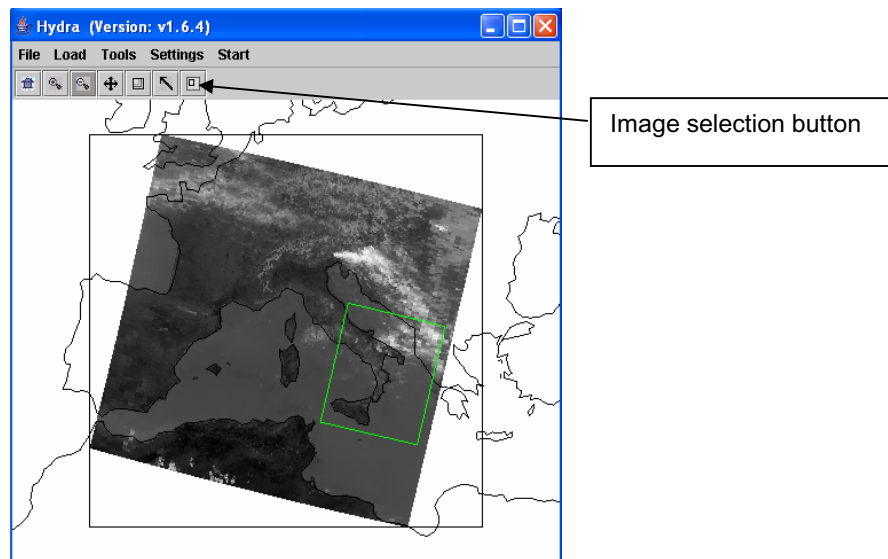
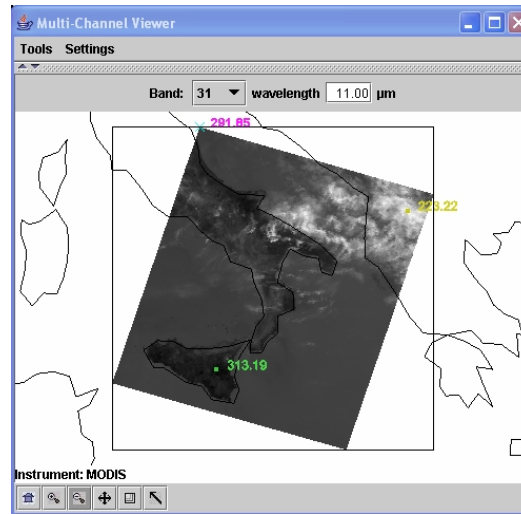


Figure 15.5: "Hydra" window showing full resolution image selection

Move the cursor over the image, and press and hold the right mouse button. Drag the cursor to select a region, and release the right mouse button. The full resolution 1km MODIS data for the area will be loaded in the “Multi-Channel viewer” window, as shown in Figure 15.6.



**Figure 15.6:** Full resolution MODIS data loaded in the “Multi-Channel viewer” window

### 15.3 Exploring the MODIS spectral bands

The Moderate Resolution Imaging Spectroradiometer (MODIS) on board the Terra and Aqua spacecraft measures radiances in 36 spectral bands between 0.645 and 14.235  $\mu\text{m}$  (King et al. 1992). Bands 1 - 2 are sensed with a spatial resolution of 250 m, bands 3 - 7 at 500 m, and the remaining bands 8 – 36 at 1000 m. The signal to noise ratio in the reflective bands ranges from 50 to 1000; the noise equivalent temperature difference in the emissive bands ranges from 0.1 to 0.5 K (larger at longer wavelengths).

Table 15.1 lists the MODIS spectral channels and their primary application. Figure 15.7 shows the spectral bands superimposed on the earth reflection and emission spectra. A summary of the some of the relevant spectral properties is presented in Figure 15.8.

**Table 15.1:** MODIS Channel Number, Wavelength ( $\mu\text{m}$ ), and Primary Application

#### *Reflective Bands*

1,2	0.645, 0.865	land/cld boundaries
3,4	0.470, 0.555	land/cld properties
5-7	1.24, 1.64, 2.13	land/cld properties
8-10	0.415, 0.443, 0.490	ocean color/chlorophyll
11-13	0.531, 0.565, 0.653	ocean color/chlorophyll
14-16	0.681, 0.75, 0.865	ocean color/chlorophyll
17-19	0.905, 0.936, 0.940	atm water vapor
26	1.375	cirrus clouds

#### *Emissive Bands*

20-23	3.750(2), 3.959, 4.050	sfc/cld temperature
24,25	4.465, 4.515	atm temperature
27,28	6.715, 7.325	water vapor
29	8.55	sfc/cld temperature
30	9.73	ozone
31,32	11.03, 12.02	sfc/cld temperature
33-36	13.335, 13.635, 13.935, 14.235	cld top properties

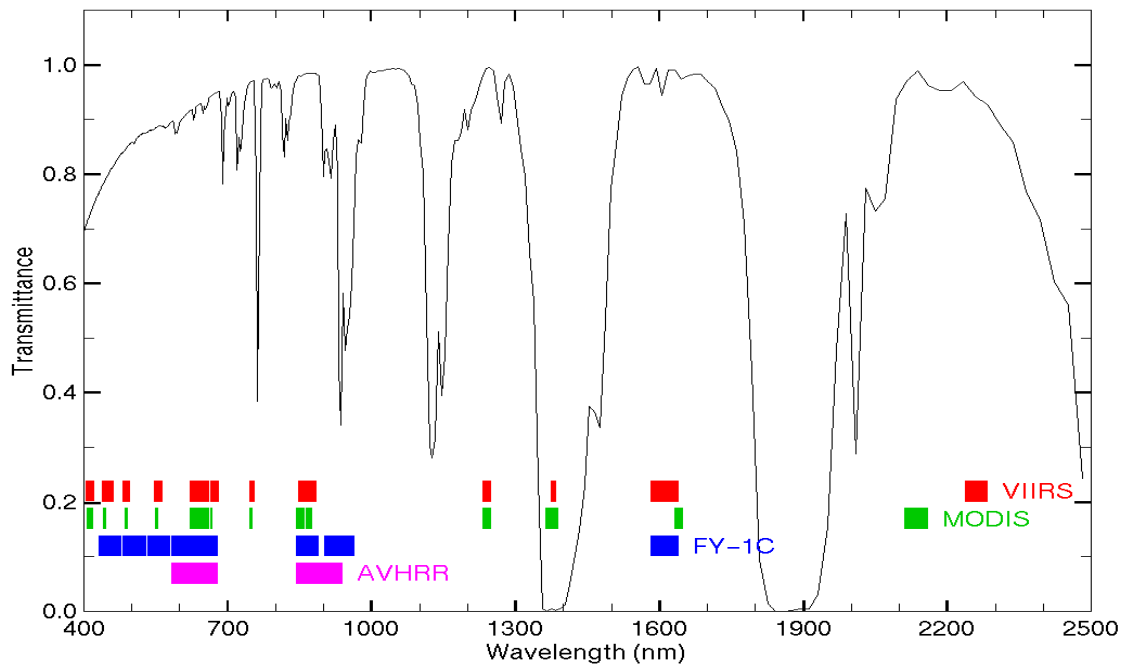
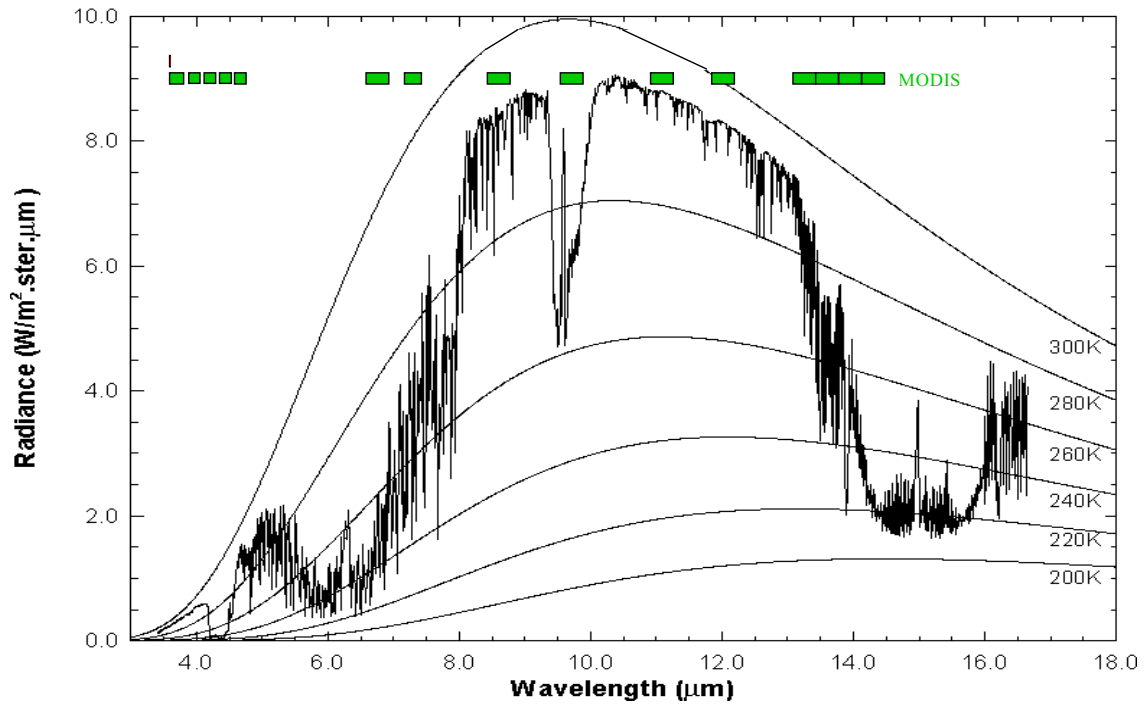


**Figure 15.7:** MODIS emissive bands superimposed on a high resolution earth atmosphere emission spectra with Planck function curves at various temperatures superimposed (top) and MODIS reflective spectral bands superimposed on the earth reflection spectra (bottom).



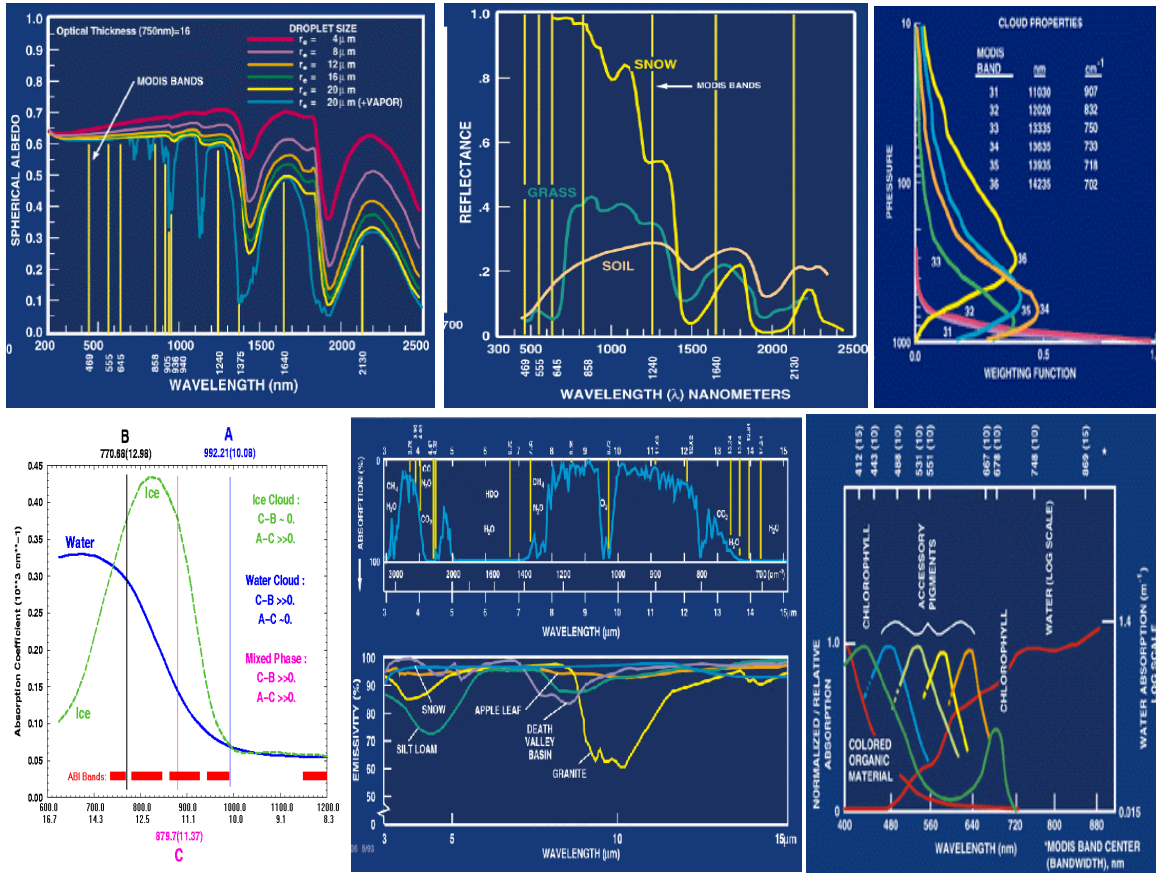


**Figure 15.8:** Summary of spectral reflectance for various surfaces between 0.3 and 2.5 μm (top left and middle), weighting functions for CO<sub>2</sub> bands (top right), water and ice cloud absorption in the LIRW region (bottom left) and atmospheric transmission and surface emissivity from 3 to 15 μm (bottom center), and water absorption of chlorophyll and accessory pigments from 0.4 to 0.9 μm (bottom right).

Using HYDRA, analyze the remote sensed measurements in a granule of MODIS data. Proceed with the following steps. Start up HYDRA and from the Hydra window. Select a data granule in hdf format (e.g. MOD021KM.A2001149.1030.003.2001154234131.hdf showing a cloud scene over Italy on 29 May 2001). Click on **Start** and then click on **Multi-channel Viewer**. Select the longwave infrared window (LIRW) **Band number** (Band 31), and display it as radiance (rather than brightness temperature) using **radiance** (under **Settings**). See Figure 15.9. Change to Brightness Temperature in the Display. Left click on the on the arrow icon on the bottom of the display and left click and drag over the image to investigate brightness temperatures at various pixels.

Show image in color by using **Set Color Scale** (under **Settings**) and click on the **color** option. Try out different color enhancement by using **Set Color Range** (under **Settings**) and changing the min and max values in the VisAD Histogram Display to 240 and 320 K. Figure 15.10 shows the resulting color enhancement. Left click on the positive magnifying glass icon on the bottom of the display and left click to magnify the scene. Left click on the negative magnifying glass icon on the bottom of the display and left click to restore the original scene.

### 15.3.1 Multi-Channel Viewer

Select a region within the image in the Multi-Channel Viewer display. Left click on the on the rubber band zoom icon on the bottom of the display (second from right) and left click drag over the

image to select a rectangular subset of the image (see Figure 15.11 for an example covering the Alps, northern Italy, and the Adriatic Sea). Investigate several spectral bands; and to notice how the cloud, atmosphere, and surface features appear in each band (not shown).

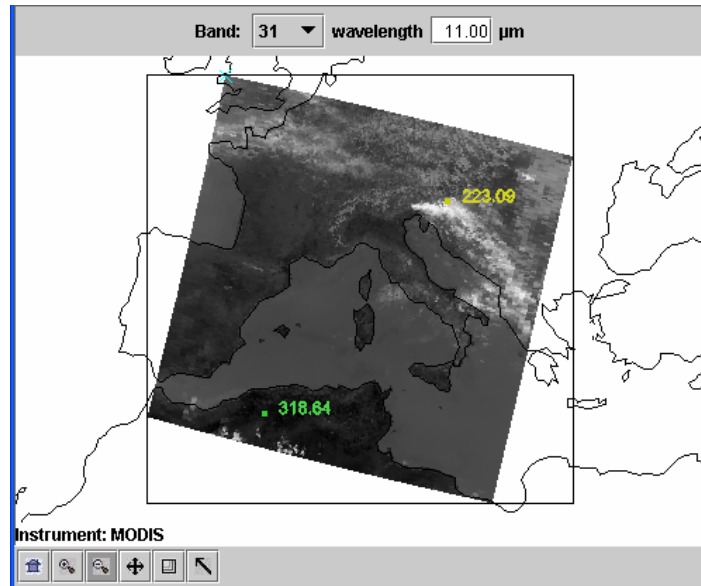


**Figure 15.9:** MODIS Display (in hydra) of MODIS IRW (Band 31) brightness temperatures (K) with minimum 223.09 and maximum 318.64 values indicated on the screen.

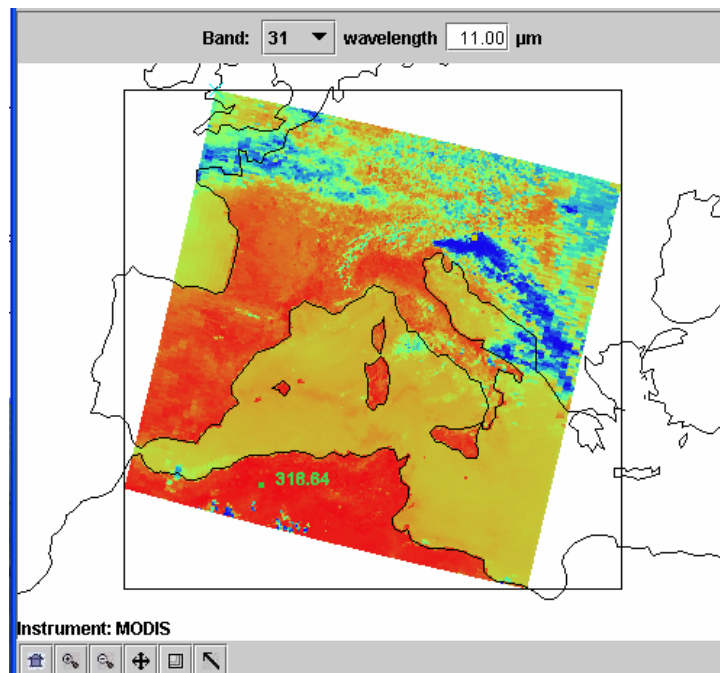


**Figure 15.10:** MODIS IRW (Band 31) brightness temperature image displayed with a color scale range from 240 K (blue) to 320 K (red).

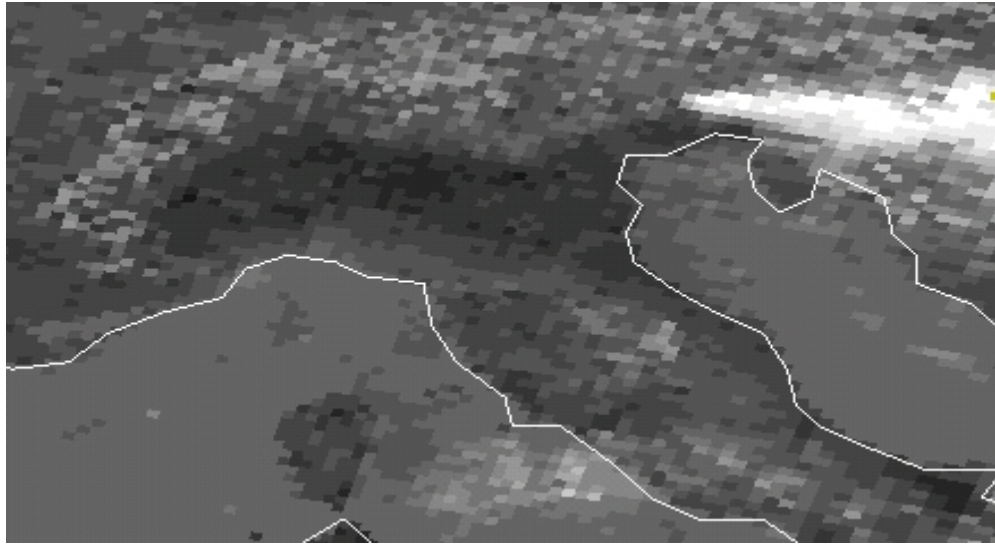


**Figure 15.11:** Selected region in Alps, northern Italy, and the Adriatic Sea.

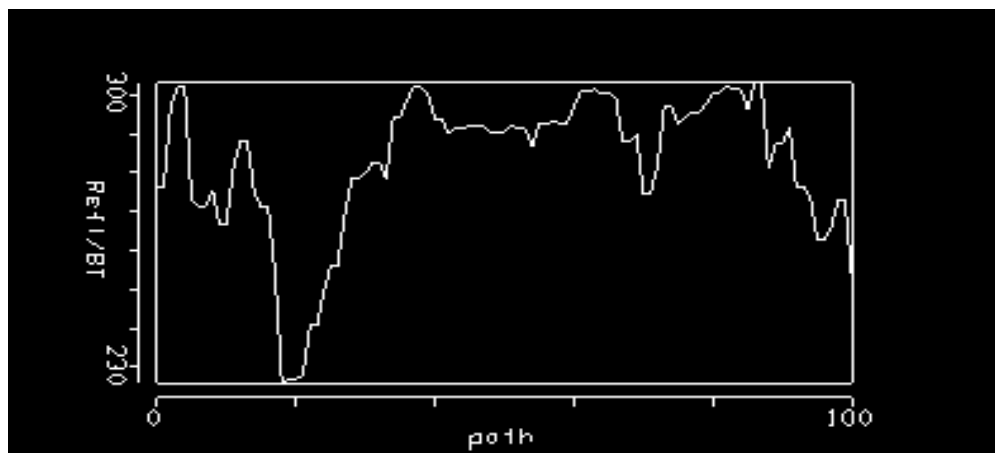
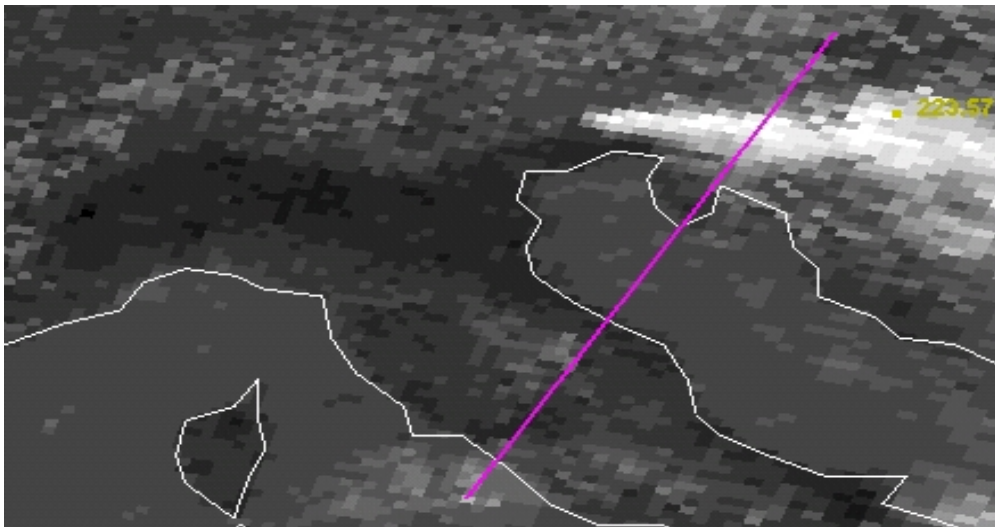


**Figure 15.12:** Brightness temperatures in Band 31 (LIRW, 11 micron) from the Alps, over the Adriatic Sea, through northern Italy, and into the Tyrranean Sea. Cloud band has BT of 230 K.

### 15.3.2 Transect

Use **Transect** (under **Tools** in the Multi-Channel Viewer display) to draw a line through the two cloud banks north-east and south-west of Italy (see Figure 15.12). To do this, left click drag. Note how the band temperatures change. Repeat this for bands 32 through 36. Note that the band temperatures are most alike in the high opaque clouds where the radiances do not transmit through very much of the atmosphere and hence do not encounter very much CO<sub>2</sub>. In the less opaque clouds (southwest of Italy) some differences in the band temperatures are noticeable. The band temperatures are most different in clear skies where transmission through the whole atmosphere must be accomplished by radiation in each spectral band; the differing CO<sub>2</sub> sensitivities of the spectral bands cause most of the radiation from each spectral band to emanate from different layers of the atmosphere. At the centre of the CO<sub>2</sub> absorption band, radiation from the upper levels of the atmosphere (e.g. radiation from below has already been absorbed by the atmospheric gas) are sensed. From spectral regions away from the centre of the absorption band, radiation from successively lower levels of the atmosphere are sensed. Away from the absorption band, the windows to the bottom of the atmosphere are found. Close this display when you are finished.

### 15.3.3 Linear Combinations

Use **Linear Combinations** (under **Tools**) to set up images that can be used in scatter plots. Create a band 31 brightness temperature image for the x-axis of the scatter plot (in the **Channel Combination Tool** display activated by **Linear Combinations** select band 31 in the red box and void the operation between the red and green boxes; use the **Compute** command on the top of the display and click on x-axis in the resulting band 31 BT image). Then create a band 31 minus band 29 image for the y-axis image (in the **Channel Combination Tool** display activated by **Linear Combinations** select band 31 in the red box and select subtraction for the operation between the red and green boxes and select band 29 in the green box; use the **Compute** command on the top of the display and click on y-axis in the resulting band 31 – band 29 BT image). With x- and y-axis displays set, return to the **Channel Combination Tool** display and activate **Scatter** on the top of the displays along a transect in the scene.

### 15.3.4 Scatter Plots

The **VisAD Scatter** display shows [BT(31)-BT(29)] versus BT(31). Display all negative values of [BT(31)-BT(29)] on the BT(31) image by left clicking on the left panel at the bottom of the **VisAD Scatter** display and left click drag to box the negative values; these appear in purple in the x-axis and y-axis images. Now display all values of [BT(31)-BT(29)] greater than 10 on the BT(31) image by left clicking on the middle panel at the bottom of the **VisAD Scatter** display and left click drag to box the values greater than 10; these appear in yellow in the x-axis and y-axis images. Finally display all values of [BT(31)-BT(29)] less than 10 and greater than 5 on the BT(31) image by left clicking on the right panel at the bottom of the **VisAD Scatter** display and left click drag to box the values between 5 and 10; these appear in turquoise in the x-axis and y-axis images.

Figure 13b shows the scatter plot and Figure 13a shows the selected regions on the BT(31) image. Note that any selected region in **VisAD Scatter** display can be erased by left clicking on the associated bottom panel followed by left click in the scatter plot, a new region can then be selected by left click drag as before. To select non rectangular regions, engage the curve toggle and left click drag enables you to draw a curve surrounding any desired points.

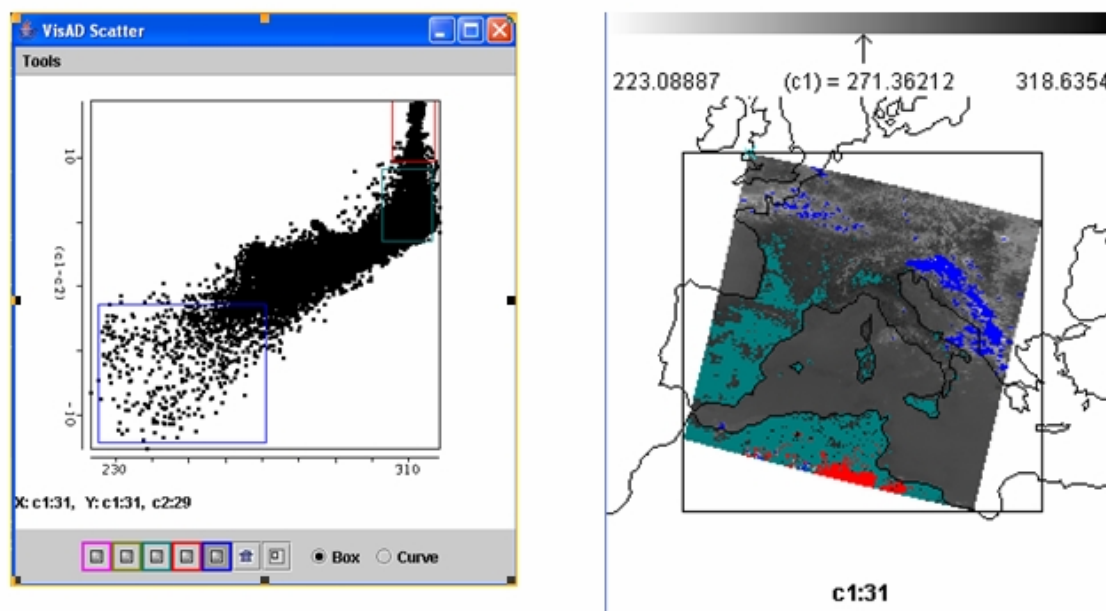


**Figure 15.13:** Scatter plot (left) of [BT31 (11  $\mu\text{m}$ )] on the x-axis and [BT31 (11  $\mu\text{m}$ ) – BT29 (8.5  $\mu\text{m}$ )] on the y-axis. Negative [BT31-BT29] indicates ice cloud in BT31 image (right).

### 15.3.5 Ice Clouds

Clear all selected regions in the in **VisAD Scatter** display (left click for each bottom panel). In the x-axis display (BT(31) image), enlarge the image by clicking on the positive magnification icon at bottom of display and then right click on the image several times. Center on the cloud in northern Italy by clicking on the cross arrows icon at the bottom of the display and then right click drag the image to the desired position. Left click drag to encircle the cloud; note that this ice cloud shows only negative values of [BT(31)-BT(29)] in the in **VisAD Scatter** display. See Figure 14.

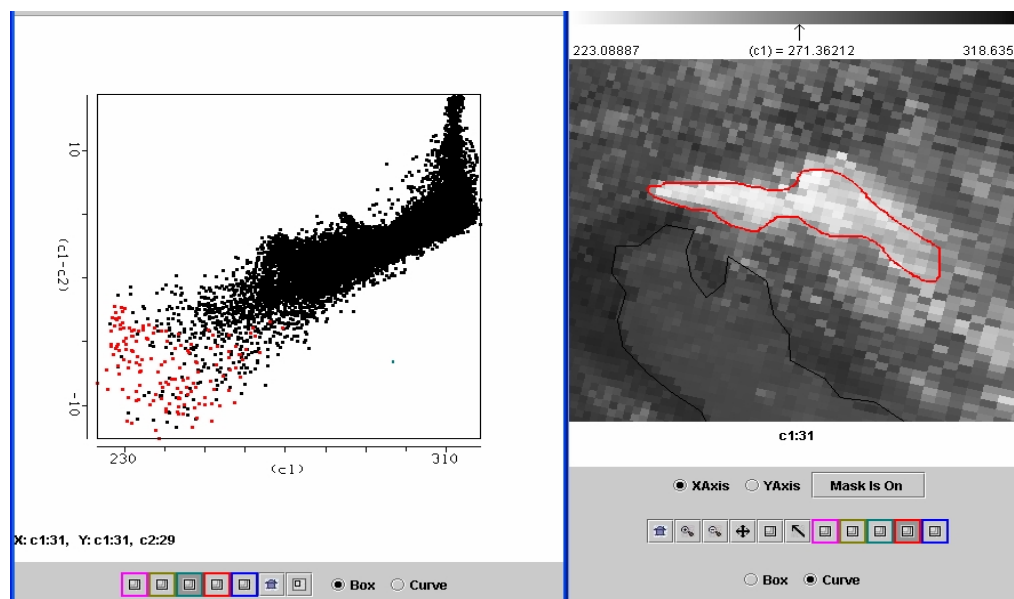


**Figure 15.14:** Scatter plot (left) of [BT31 (11  $\mu\text{m}$ )] on the x-axis and [BT31 (11  $\mu\text{m}$ ) – BT29 (8.5  $\mu\text{m}$ )] on the y-axis. Cloud in BT31 image (right) shows negative [BT31-BT29] values in scatter plot, suggesting ice cloud.

### 15.3.6 SIRW and LIRW

Explore scatter plots of BT(21) versus BT(31). Select some cloud and some clear surface. Note that BT(SIRW) values are warmer than BT(LIRW) in cloudy scenes but they are roughly the same over non-vegetated land.

### 15.3.7 Water Vapor Channel

Select **Band 27** ( $6.7 \mu\text{m}$ ) on the Multichannel Viewer Display. This WV band is used in cloud detection but also to derive upper tropospheric humidity (UTH). A dry slot is evident in the  $6.7 \mu\text{m}$  (band 27) water vapor sensitive image and upper level opaque clouds are apparent toward the northwest. Draw a transect over the dry slot and note the 10 K BT(27) increase. See Figure 15.15.

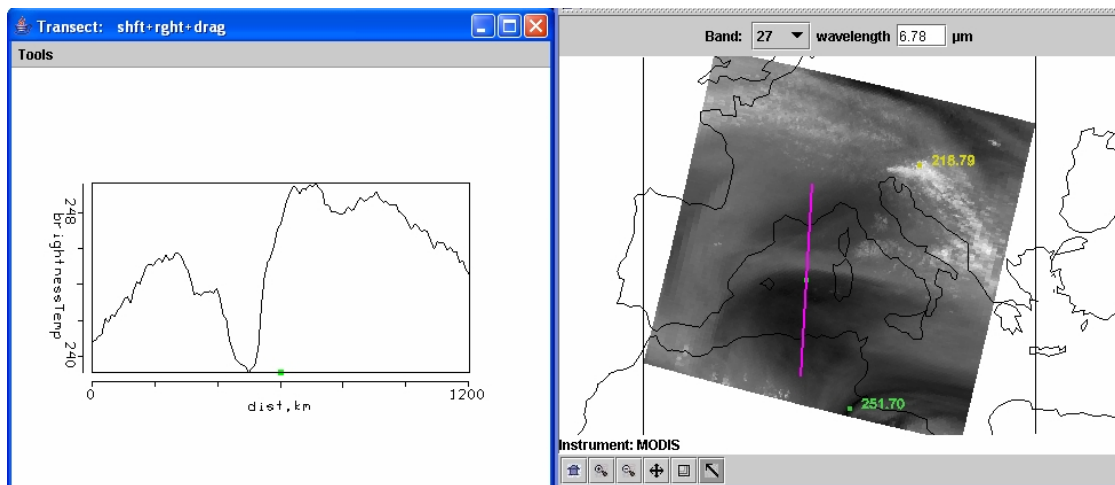


**Figure 15.15:** Cross-section plot (left) of BT(H<sub>2</sub>O) for the  $6.7 \mu\text{m}$  (band 27) water vapor sensitive band (right) from north to south over a dry slot. The dry slot is about 10 C warmer than the neighboring wet areas.

### 15.3.8 NIR

Explore the bands 1 ( $0.65 \mu\text{m}$ ), 6 ( $1.64 \mu\text{m}$ ), and 31 ( $11 \mu\text{m}$ ) measurements over the Alps, northern Italy, and the Adriatic Sea. Demonstrate how the low  $1.6 \mu\text{m}$  reflectance in Alpine snow contrasts with high  $1.6 \mu\text{m}$  reflectance in ice clouds helping to distinguish between the two. See Figure 15.16.

### 15.3.9 Surface and cloud features

Combine spectral bands that are useful for characterizing surface and cloud features. Plot the band combination [band 2 ( $0.86 \mu\text{m}$ ) / band 1 ( $0.65 \mu\text{m}$ )] on the y-axis and band 31 ( $11 \mu\text{m}$ ) on the x-axis is shown in Figure 15.17. Select points in the scatter plot to reveal that clouds are found when the band ratio (2/1) is near one and band 31 is cold and non-vegetated land appears when the band ratio (2/1) is near one and band 31 is hot. Vegetated land appears when the band ratio is much greater than 1. Investigate how the snow index [band 1 ( $0.65 \mu\text{m}$ ) – band 6 ( $1.6 \mu\text{m}$ ) / band 1 ( $0.65 \mu\text{m}$ ) + band 6 ( $1.6 \mu\text{m}$ )] helps to distinguish snow (near one) from clouds (near zero). Warmer surface temperatures with snow index near one are sometimes outlining ocean features.

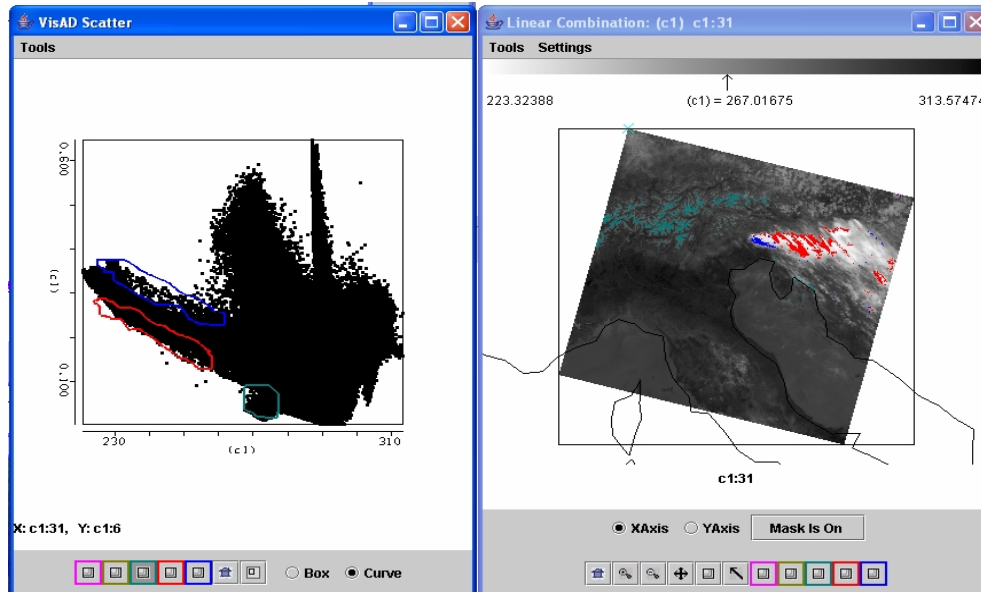


**Figure 15.16:** Scatter plot (left) of reflectance in 1.6  $\mu\text{m}$  (band 6) versus brightness temperature in 11  $\mu\text{m}$  (band 31). BT(31) image (right) shows snow in Alps (green) is distinguished from smoke (blue) and ice red) in clouds by differing band 6 reflectances.

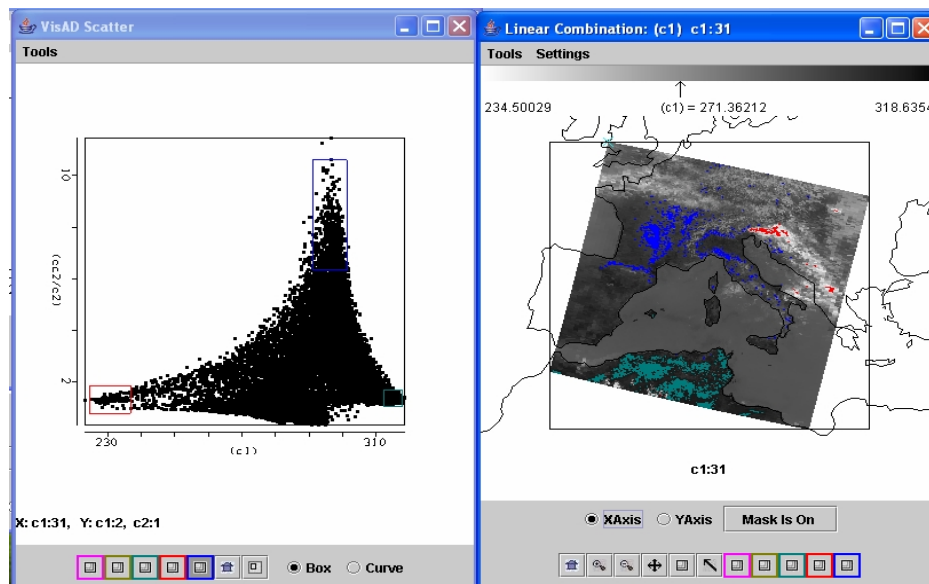


**Figure 15.17:** Scatter plot (left) of brightness temperature in 11  $\mu\text{m}$  (band 31) vs reflectance ratio 0.8/0.6  $\mu\text{m}$  (band 2 / band 1). BT(31) image (right) shows clouds (red with b2/b1 close to one and BT31 cold), non-vegetated land (green with b2/b1 close to one and BT31 hot), and vegetated land (blue with b2/b1 much greater than one and BT31 warm).

## 15.4 Detecting Clouds

### 15.4.1 Spectral band combinations for cloud detection

Cloud detection can be refined using spectral band combinations that include 0.65, 0.85, 1.38, 1.6, 8.6, and 11  $\mu\text{m}$ . Multispectral investigation of a scene can separate cloud and clear scenes into various classes. Cloud and snow appear very similar in a 0.65  $\mu\text{m}$  image, but dissimilar in a 1.6  $\mu\text{m}$  image (Figure 15.8 indicates that snow reflects less at 1.6 than 0.65  $\mu\text{m}$ ). For 8.6  $\mu\text{m}$

ice/water particle absorption is minimal, while atmospheric water vapor absorption is moderate. For  $11\mu\text{m}$ , the opposite is true. Using these two bands in tandem, cloud properties can be distinguished. Large positive values of  $[\text{BT}8.6 - \text{BT}11]$  indicate the presence of cirrus clouds; negative differences indicate low water clouds or clear skies. Cloud boundaries are often evident in local standard deviation of radiances. The  $1.38\mu\text{m}$  offers another opportunity to detect high thin cirrus; this channel images the upper troposphere and is highly sensitive to the presence of ice crystals.

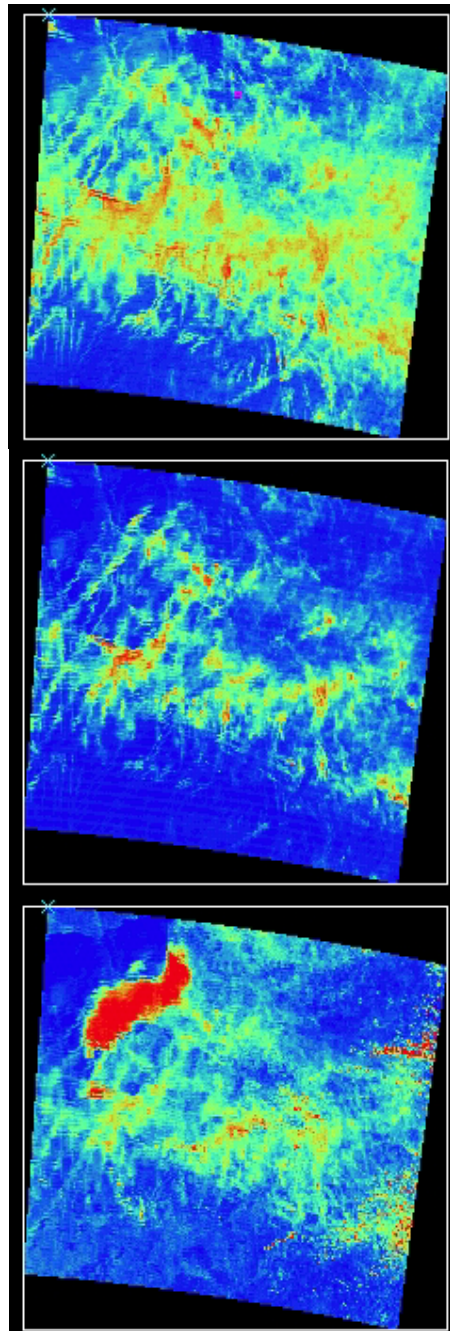


**Figure 15.18:** Contrails seen in (top) positive values of  $[\text{BT}(8.6) - \text{BT}(11)]$  in yellow and red, (middle) high reflectance in  $[r(1.38)]$ , and (bottom) high reflectance in  $[r(0.6)]$ . Some of the contrails are not seen in the visible.

Focus on the thin cloud region in the northwest corner of the image. View band 31 ( $11\mu\text{m}$ ) versus  $[\text{band } 29 (8.6\mu\text{m}) - \text{band } 31 (11\mu\text{m})]$ . Figure 15.18 shows that the largest positive



differences are found in ice clouds and negative differences occur in water clouds. Band 26 (1.38  $\mu\text{m}$ ) confirms the contrail locations; it is sensitive to water and ice reflectances from the upper half of the troposphere. Some of these clouds are not evident in the visible image at 0.65  $\mu\text{m}$ .

#### 15.4.2 Tri-spectral IR Windows

Select a small region within the cloud band northeast of Italy. Plot the brightness temperature differences [band 29 (8.6 $\mu\text{m}$ ) - band 31 (11 $\mu\text{m}$ )] on the x-axis and [band 31 (11 $\mu\text{m}$ ) - band 32 (12 $\mu\text{m}$ )] on the y-axis (see Figure 19). Note the hook shaped scatter plot resulting from partially clear and cloud contributions to the brightness temperature in each spectral band. The Planck function radiance at shorter wavelengths is dependent on temperature to a higher power than the Planck radiances at longer wavelengths, thus the warmer part of the pixel contributes more to the brightness temperature at shorter wavelengths.

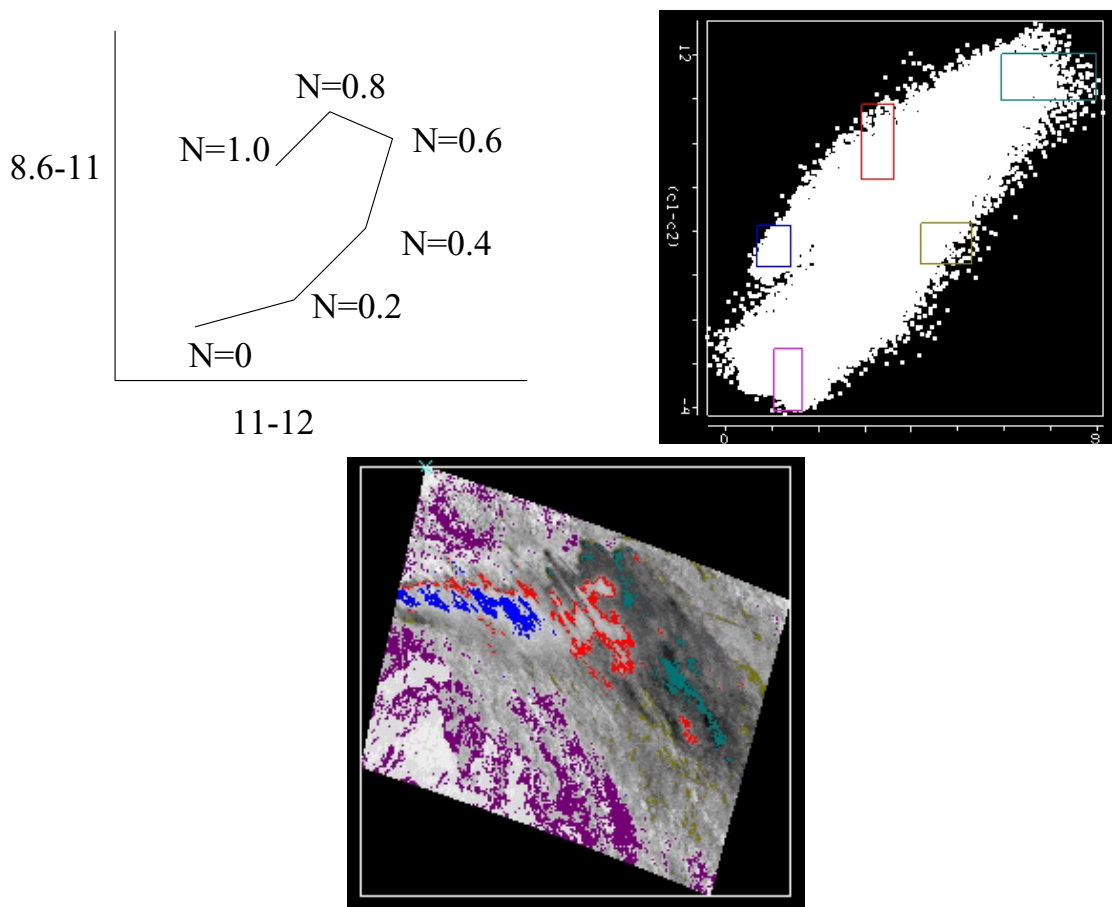


**Figure 15.19:** (top left) diagram of [BT(8.6)-BT(11)] versus [BT(11)-BT(12)] as a function of cloud fraction; (top right) scatter plot of [BT(8.6)-BT(11)] versus [BT(11)-BT(12)] for cloud scene on 29 May 2001, (bottom) subsets of scatter plot colored onto image of [BT(11)-BT(12)] demonstrating concept of top diagram.

To see this more clearly consider a calculation for broken clouds. Assume  $T_{\text{clr}}=300$  and  $T_{\text{cld}}=230$ . Recalling the discussion in Chapter 2 on temperature sensitivity of the Planck function,  $\text{dB}/B = \alpha \text{ d}T/T$  where  $\alpha \approx c_2\nu/T$  implies that  $B$  is proportional to  $T^\alpha$ . Thus the cold part of pixel has more influence at longer wavelengths (lower wavenumbers).

$$B_{12} \approx (1-N)T_{\text{clr}}^{4.1} + N T_{\text{cld}}^{2.8} \sim (1-N)300^{4.1} + N 200^{2.8}$$

$$B_{11} \approx (1-N)T_{\text{clr}}^{4.3} + N T_{\text{cld}}^{2.9} \sim (1-N)300^{4.3} + N 200^{2.9}$$

$$B_{8.6} \approx (1-N) \cdot T_{clr}^{5.6} + N \cdot T_{cld}^{3.7} \sim (1-N) \cdot 300^{5.6} + N \cdot 200^{3.7}$$

Then when the brightness temperature differences in the scatter plot are considered,

$$\begin{aligned} [BT_{11}(N) - BT_{12}(N)] &= [(1-N) \cdot B_{11}(T_{clr}) + N \cdot B_{11}(T_{cld})]^{-1} - [(1-N) \cdot B_{12}(T_{clr}) + N \cdot B_{12}(T_{cld})]^{-1} \\ [BT_{8.6}(N) - BT_{11}(N)] &= [(1-N) \cdot B_{8.6}(T_{clr}) + N \cdot B_{8.6}(T_{cld})]^{-1} - [(1-N) \cdot B_{11}(T_{clr}) + N \cdot B_{11}(T_{cld})]^{-1} \end{aligned}$$

we find that as we move from clear ( $N=0$ ) to cloudy ( $N=1$ ) skies they arrange themselves in a hook shape (see Figure 19). The spectral dependence of the cloud emissivity will modify the results of this simple calculation somewhat, but the dominating influence is from the Planck function.

This also demonstrates why cloud edges introduce difficulties to cloud detection techniques that rely on threshold brightness temperature differences to indicate cloud presence.

### 15.5 Mapping Vegetation

The vegetation index is based on the relatively low leaf and grass reflectance from spectral bands below  $0.72 \mu\text{m}$  and relatively high reflectance from spectral bands above. Construct a pseudo image of normalized vegetation index  $[\text{band } 2 (0.86 \mu\text{m}) - \text{band } 1 (0.65 \mu\text{m})] / [\text{band } 2 (0.86 \mu\text{m}) + \text{band } 1 (0.65 \mu\text{m})]$ . Figure 20 shows that regions with some vegetation are clearly distinguished from those with little. Regions without significant vegetation have indices below 0.3; vegetated regions show indices above 0.6.

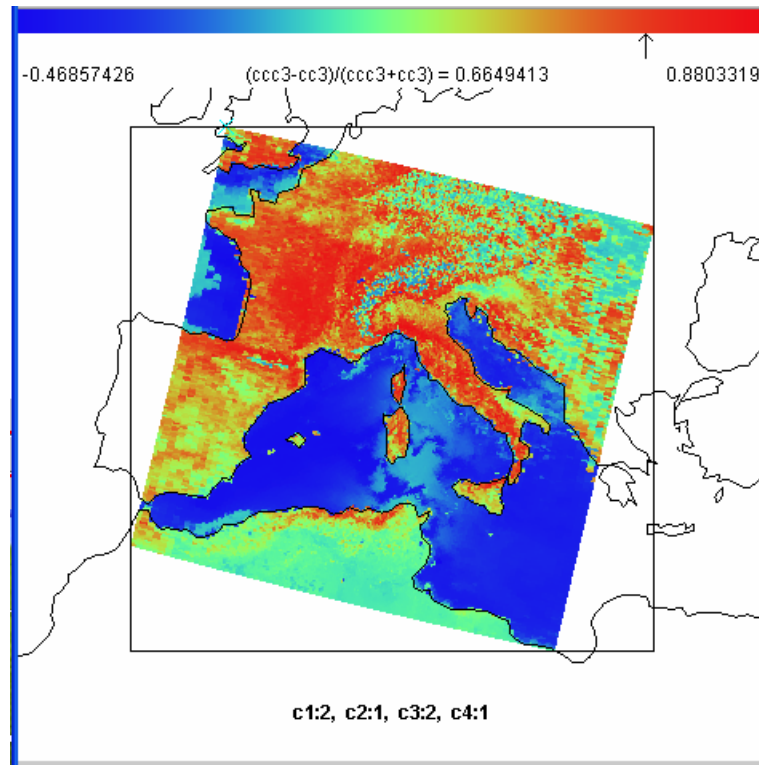


**Figure 15.20:** A pseudo image of normalized vegetation index  $[\text{band } 2 (0.86 \mu\text{m}) - \text{band } 1 (0.65 \mu\text{m})] / [\text{band } 2 (0.86 \mu\text{m}) + \text{band } 1 (0.65 \mu\text{m})]$ . Regions with some vegetation are clearly distinguished from those with little. Dry desert-like regions on the heel of Italy and in northern Africa show vegetation indices below 0.3; fertile valleys in northern Italy show indices above 0.8.

### 15.6 Investigating a Volcanic Eruption

MODIS measurements of a volcanic eruption of Mt Etna on 28 October 2002 are found in file MOD021KM.A2002301.1215.003.2002302200901.hdf. Select Region to focus on the eruption (see Figure 15.21). Figure 15.21 shows the scatter plot of [Band 31 - Band 32] on the y-axis and Band 31 (11  $\mu\text{m}$ ) on the x-axis. The volcanic ash produces negative temperature differences (between 0 and  $-6$  C) in the split window; the denser ash produces the larger differences.

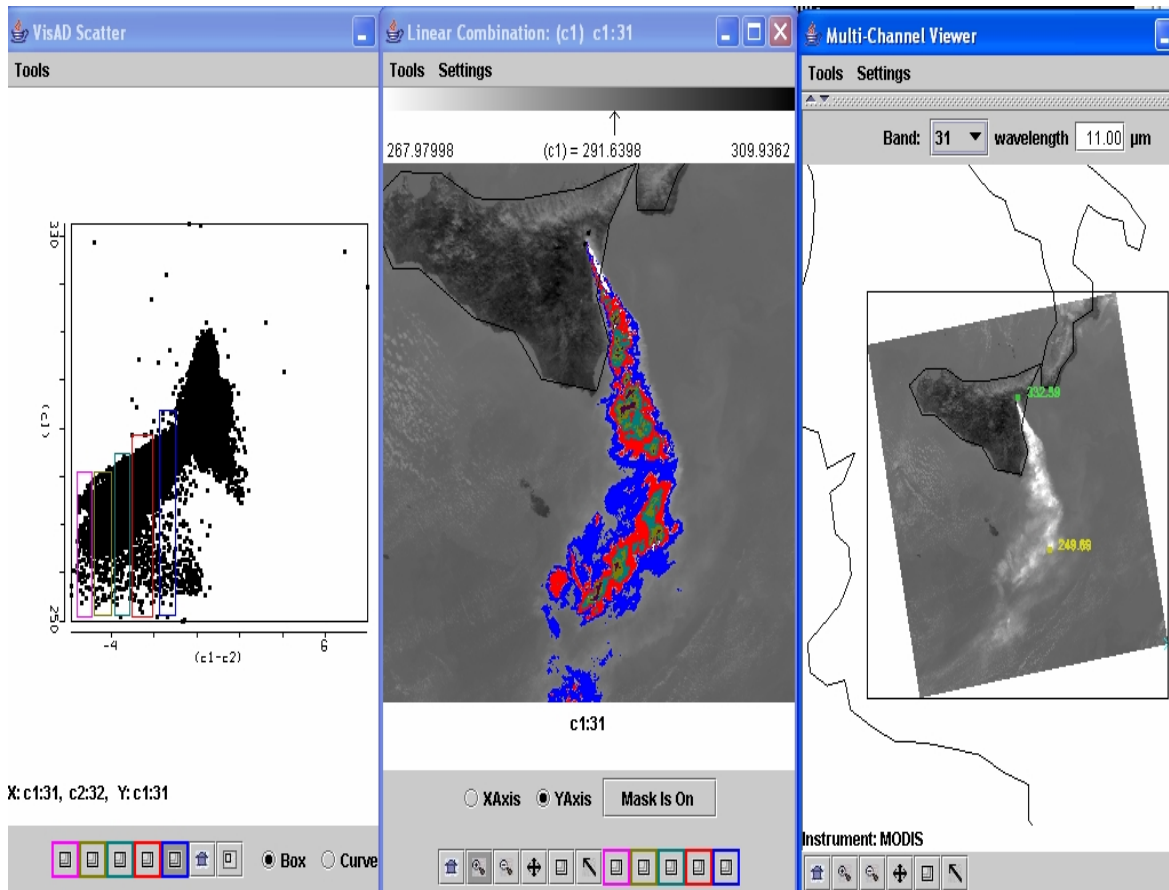


**Figure 21:** (right) Infrared window image of [band 31 (11 $\mu\text{m}$ )] of Mt Etna eruption on 28 Oct 2002; (middle) color enhanced image of [band 31 (11 $\mu\text{m}$ ) - band 32 (12 $\mu\text{m}$ )] with blue, red, green, olive, and purple indicating progressively larger BT differences from 0 to  $-6$  C; and (left) scatter plot of [band 31 (11 $\mu\text{m}$ ) - band 32 (12 $\mu\text{m}$ )] on the x-axis and band 31 (11 $\mu\text{m}$ ) on the y-axis. The larger differences come from the denser ash.

### 15.7 Investigating Coastal Waters (SST and Chlorophyll)

MODIS measurements of Western Australia on 19 August 2000 can be found in MOD021KM.A2000232.0300.004.2002365101900.hdf. Focusing on the Shark Bay region, Figure 15.22 shows a pseudo image of the sea surface temperature derived from band 31 (11 $\mu\text{m}$ ); it is obvious that the waters within Shark Bay are much cooler than the Leeuwin current waters along the WA coastline. Figure 15.22 also shows a scatter plot of band 31 (11 $\mu\text{m}$ ) on the x-axis and (band 9 (0.44 $\mu\text{m}$ ) / band 12 (0.57 $\mu\text{m}$ )) on the y-axis. Band 9 has relatively high and band 12 has relatively low water absorption for chlorophyll; the low ratio values are an indication of chlorophyll concentrations.

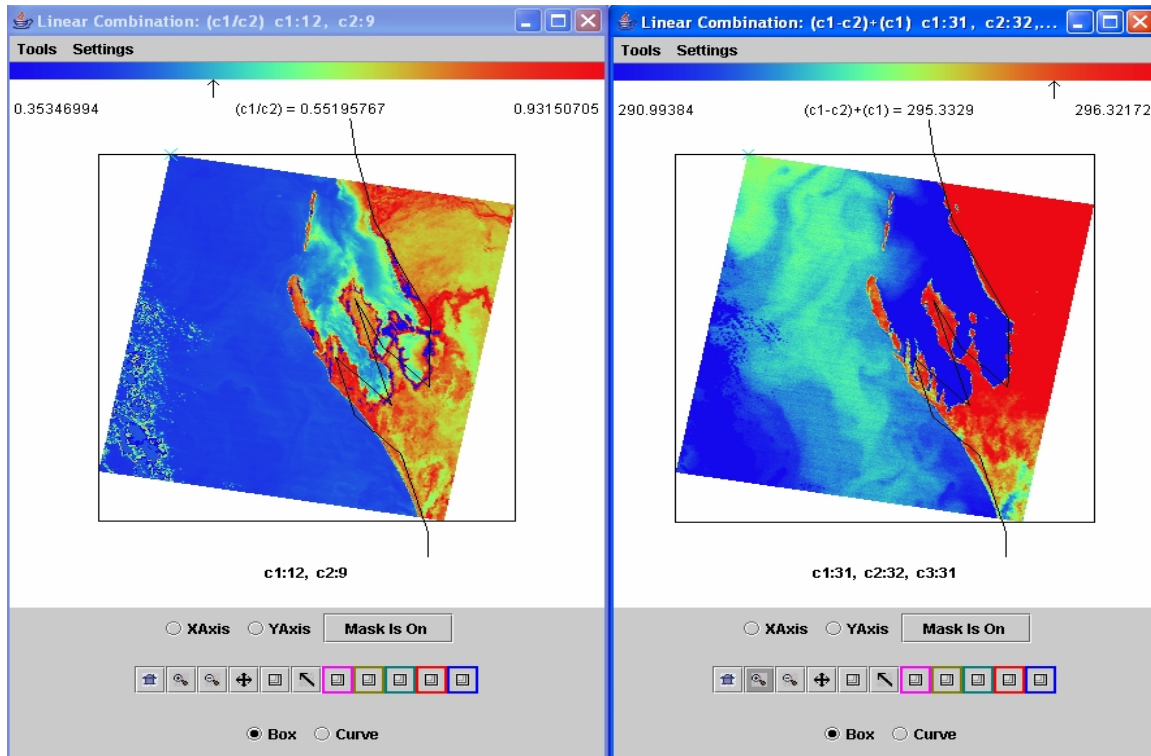


**Figure 15.22:** (right) Image of sea surface temperature estimated by  $[2 \cdot BT(11) - BT(12)]$  showing waters within Shark Bay (blue) are about 4 C cooler than the Leeuwin current waters (turquoise) along the WA coastline. (left) Image indicative of chlorophyll concentrations in Shark Bay estimated by band 12 ( $0.57\mu\text{m}$ ) / band 9 ( $0.44\mu\text{m}$ ) where high ratio values are an indication of more chlorophyll.

### 15.8 Summary

New multispectral sensors such as MODIS, MERIS, GLI, and MSG are capable of producing a variety of enhanced products that include (a) cloud detection, (b) aerosol concentration and optical properties during the day, (c) cloud optical thickness, thermodynamic phase, and top temperature, (d) vegetation and land surface cover, (f) snow and sea-ice cover, and (g) surface temperature. These capabilities will be continued into the future with VIIRS, ABI, MTSAT-R, and others.